

Numerical Investigation of the Online Parameter Estimation Techniques for Interior Permanent Magnet Synchronous Machines

Bui Xuan Minh^{1*}, Le Khắc Thủy¹, Le Minh Kien¹, Nguyen Trung Kien¹, Nguyen Thanh Tien¹, Pham Xuan Phuong¹

¹ Le Quy Don Technical University, Ha Noi, Vietnam

*Corresponding author E-mail: minh.buixuan@ieee.org

Abstract

This paper presents a new method to estimate online four parameters of the interior permanent magnet synchronous motors (IPMSM), including stator resistance, d- axis inductance, q-axis inductance and permanent magnet flux linkage. The proposed method is based on the neural network with the training data taken from experiments, which were preprocessed before feeding to the input of the neural network model. The proposed online parameters estimation method is evaluated by comparing the estimation accuracy and the updating time with other conventional online methods, such as Extended Kalman Filter, Recursive Least Square and the Adaline Neural Network. Extensive numerical simulations have been conducted to verify the effectiveness and the accuracy of the proposed method.

Keywords: IPMSM, Online Parameter Identification, Neural Network, Kalman Filter, Recursive Least Square

Symbols

Symbols	Units	Description
Ψ_m	Wb	Rotor flux linkage
R	Ω	Stator resistance
L_d, L_q	H	d and q stator inductance
i_d, i_q	A	d and q stator current
v_d, v_q	V	d and q stator voltage
ω	Rad/s	Electrical angular speed of the rotor

Abbreviations

IPMSM	Interior Permanent Magnet Synchronous Machines
RLS	Recursive Least Square
EKF	Extended Kalman Filter
ANN	Adaline Neural Network
FOC	Field Oriented Control
DTC	Direct Torque Control
MPC	Model Predictive Control

1. Introduction

Due to high power density and efficiency, Interior Permanent Magnet Synchronous Motors (IPMSMs) find various applications such as in wind generator, CNC machine and electric/ hybrid electric vehicles (EV/HEV) [1]. Identifying machine parameters is significant in control strategies, for example, in field-oriented control (FOC), direct torque control (DTC) and model predictive control (MPC). Determining parameters is required to ensure a stable system while improving its efficiency and dynamic response. Especially, in vector-control methods, the parameters of a PI controller, which affects the control performance of the IPMSM drive system, are determined using the IPMSM parameters [2]. As a result, the more accurate IPMSM parameters identified, the better control over the drive system can be achieved. In addition to that, as the IPMSM is associated with potential issues such as demagnetization due to temperature rise or inter-turn short circuit (ITSC) in stator windings, condition monitoring is necessary to ensure the safe and correct operation of the IPMSM, which can be done by tracking the IPMSM parameters. For example, in [3], a technique was proposed to estimate the stator resistance and flux linkage to online monitor the working conditions of rotor permanent magnet (PM) and stator winding. In general, there are two types of

parameter identification, which are online and offline techniques to be reviewed as follows.

Regarding offline techniques, the input/output data need to be collected first, then from which the IPMSM parameters can be estimated when the IPMSM is not connected with a load or at standstill state. The finite element analysis (FEA) is the offline technique, which requires the details of IPMSM design, structural and geometric information to calculate its parameters [4]. FEA can capture the effects of mutual inductances and the change in magnetic flux due to magnetic saturation [5]. However, if the required information is not acquirable, FEA cannot be implemented. Another offline technique is Standard Standstill Frequency Response test (SSFR test), in which the test signals driven by Voltage Source Inverter (VSI) are injected into the IPMSM. SSFR test can give high accurate identified parameters but measuring instruments are required [6]. The downside of SSFR test also stems from the fact that its identified parameters are distorted by VSI nonlinearities. At standstill state, the step DC voltage excitation tests can be used to identify apparent inductance without accurately capture the magnetic saturation effect [7]. Meanwhile, in dq-axis square voltage excitation tests [8], more parameters can be estimated such as stator resistance, rotor flux linkage and initial rotor position, but magnetic saturation effect is not considered, still. The technique in [9] can account for the effects of self-and-cross magnetic saturation, which can identify flux linkages from the measured dq-axis currents at constant rotor speed. Afterwards, by taking the partial derivatives of dq-axis flux linkages over currents, the incremental inductances can be found. In general, offline techniques cannot identify the flux linkage and resistance, which vary with time during the real-time operation of IPMSM; therefore, they cannot be used for online IPMSM parameter tracking.

Meanwhile, an online technique refers to estimating parameters during the operation of the IPMSM, which are updated in real-time given new input/output data. During the operation of the IPMSM, the temperature will increase, resulting in the increase in stator resistance and the decrease in flux linkage, accordingly. Therefore, by knowing these real-time dependent parameters, the thermal states of the IPMSM can be monitored [10], [11], which, in turn, serves diagnosis purposes related to the damage of winding insulation and demagnetization. Online parameter identification includes observer-based techniques, such as in [12] in which a method for bearing fault diagnosis is proposed with the peak energy spectrum introduced into the flux linkage observer. Further, in [13], an interturn short circuit fault detection is proposed based on residual current vector (RCV), which is generated by the difference between the measured stator currents and the estimated stator currents from a state observer. On the other hand, many sensorless identification techniques have been proposed to overcome the limitation of mechanical sensors and their costs involved in the implementation of the drive system. Due to the advance in high-performance computing technology, AI-based techniques have been employed to monitor the thermal states of winding and PM as in [14], which uses neural network (NN) for identification. In addition to NN algorithms, extended Kalman Filter (EKF), model reference adaptive system (MRAS) and recursive least square (RLS) are usually used to design parameter estimators. In [15], a technique based on EKF is proposed

to estimate winding resistance and rotor flux linkage, and the results show that it is not stable and subject to noise. RLS techniques utilizes the injection of square wave current signal [16] or sinusoidal current signals [17] to solve the rank deficiency problems when estimating four parameters with only two available equations. The disadvantages of these methods are that the injected current signals produce the current and torque ripples and that estimation accuracy is low due to the non-linearity of the power converters. The other weakness of these methods is the slow update capability during the nature of recursive algorithm. Results in [18] show that MRAS, which identifies stator resistance and rotor flux linkage, is sensitive to disturbances. Further, it is also time-consuming to fine-tune the parameters of its adaptive mechanism.

This paper proposes a solution to estimate four IPMSM parameters, including dq-axis inductances, rotor flux and stator winding resistance, based on Artificial Neural Network method. The main novelty of the proposed method is that four neural network models were trained to estimate four different parameters and that the subsequent estimation of q-axis inductance, stator resistance and d-axis inductance, rotor flux linkages result in the improvement of the estimation accuracy and fast updating capability. Furthermore, the input of every neural network model was proposed to be the function of the measured variables, which significantly affect the variation of the specific estimated parameter. As a result, the training time and the computation burden of the estimator can be reduced. In addition, an IPMSM drive system implemented in MATLAB/Simulink is used to compare and evaluate the proposed solution together with EKF, RLS and Adaline NN. The rest of this paper is arranged as follow. The next section outlines mathematical expressions related to the IPMSM model, three mentioned estimation techniques as well as the proposed solution. The third section presents the simulation setup and results with discussion to highlight the superiority of the proposed solution over the other techniques. Finally, the conclusion is presented in the fourth section.

2. Online parameters identification methods

2.1. IPMSM model

Assuming that the cross-coupling effect is negligible, the dq-axis equations of the PMSM are given by:

$$\frac{di_d}{dt} = -\frac{R}{L_d}i_d + \frac{L_q}{L_d}\omega i_q + \frac{u_d}{L_d} \quad (1a)$$

$$\frac{di_q}{dt} = -\frac{R}{L_q}i_q - \frac{L_d}{L_q}\omega i_d + \frac{u_q}{L_q} - \frac{\psi_m}{L_q}\omega \quad (1b)$$

where i_d , i_q , u_d and u_q are the dq-axis stator currents and voltages, respectively. ω denotes the electrical angular speed. R , L_q , L_d and ψ_m are the stator resistance, q-axis inductance, d-axis inductance, and rotor flux linkage, respectively. In this paper, before estimation, low-pass filters (LPFs) will be applied to measured data, which include i_d , i_q , u_d , u_q and ω . After filtering, the steady-state IPMSM model will be discretized as:

$$u_d(k) = R(k)i_d(k) - L_q(k)\omega(k)i_q(k) \quad (2a)$$

$$u_q(k) = R(k)i_q(k) + L_d(k)\omega(k)i_d(k) + \psi_m(k)\omega(k) \quad (2b)$$

2.2. Recursive Least Square method

The mathematical model of a RLS algorithm is:

$$y_k = \Phi_k^T x \quad (3)$$

where x is the unknown parameters to be estimated, Φ_k and y_k denote the input and output of the system, respectively. The update rule for RLS is:

$$\begin{aligned} \hat{x}_{k+1} &= \hat{x}_k + G_{k+1}[y_{k+1} - \Phi_{k+1}^T \hat{x}_k] \\ G_{k+1} &= P_k \Phi_{k+1}^T [I\lambda + \Phi_{k+1}^T P_k \Phi_{k+1}]^{-1} \\ P_{k+1} &= (P_k - G_{k+1} \Phi_{k+1}^T P_k) / \lambda \end{aligned} \quad (4)$$

where I is the identity matrix; λ is the forgetting factor; G_k and P_k the gain and covariance matrices, respectively. The RLS algorithm can be implemented to estimate dq-axis inductance, the corresponding model will be:

$$x = \begin{bmatrix} L_q \\ L_d \end{bmatrix}, \Phi = \begin{bmatrix} -\omega(k)i_q(k) & 0 \\ 0 & \omega(k)i_d(k) \end{bmatrix} \quad (5)$$

$$y = \begin{bmatrix} u_d(k) - Ri_d(k) \\ u_q - Ri_q(k) - \psi_m \omega(k) \end{bmatrix} \quad (6)$$

2.3. Extended Kalman Filter

The EKF algorithm is an extended version of Kalman Filter, which deals with non-linear problem. The system model for EKF is expressed as:

$$\begin{aligned} x_{k+1} &= F_k(x_k, u_k) + w_k \\ y_k &= H(x_k) + v_k \end{aligned} \quad (7)$$

In which $x_k = [i_d \ i_q \ p_1 \ p_2]^T$ is the state vector, where p_1 and p_2 are two arbitrary machine parameters. $y_k = [i_d \ i_q]^T$ is the system output. $u_k = [u_d^* \ u_q^*]$ is the control input. w_k (system noise) and v_k (measurement noise) are zero-mean white Gaussian noises with covariance matrices Q and R , respectively. $F_k(x_k, u_k)$ and $H(x_k)$ denote the prediction and transformation functions, respectively. Further, the discrete system function F_k is show in (8). The EKF recursively finds the optimal state estimate $\hat{x}_{k|k}$ as the mean of the normal distribution represented by the covariance matrix $P_{k|k}$.

$$F_k = \begin{bmatrix} i_{d,k} \left(1 - \frac{R}{L_d} T_s\right) + \frac{L_q}{L_d} \omega i_{q,k} T_s + \frac{u_d}{L_d} T_s \\ i_{q,k} \left(1 - \frac{R}{L_q} T_s\right) - \frac{L_d}{L_q} \omega i_{d,k} T_s + \frac{u_q}{L_q} T_s - \frac{\phi_m}{L_q} T_s \\ p_1 \\ p_2 \end{bmatrix} \quad (8)$$

The EKF starts with predicting the new state vector given the previous estimation consisting of $\hat{x}_{k-1|k-1}$ with $P_{k-1|k-1}$ and u_{k-1} .

$$\begin{aligned} \hat{x}_{k|k-1} &= F_k(\hat{x}_{k-1|k-1}, u_{k-1}) \\ P_{k|k-1} &= F_{k-1} P_{k-1|k-1} F_{k-1}^T + Q \end{aligned} \quad (9)$$

$$\text{where } F_{k-1} = \frac{\partial F_k(\hat{x}_{k-1|k-1}, u_{k-1})}{\partial \hat{x}}$$

Then, in the second step, EKF will correct the prediction using the most recent measurement, which is expressed as:

$$\begin{aligned} K_k &= P_{k|k-1} H_k^T (H_k P_{k|k-1} H_k^T + R)^{-1} \\ \hat{x}_{k|k} &= \hat{x}_{k|k-1} + K_k (y_k - H(\hat{x}_{k|k-1})) \\ P_{k|k} &= P_{k|k-1} - K_k H_k P_{k|k-1} \end{aligned} \quad (10)$$

where $H_k = \frac{\partial H(\hat{x}_{k|k-1})}{\partial \hat{x}}$, y_k is the measured output and K_k is the Kalman gain.

2.4. Adaline Neural Network

The mathematical model of an Adaline Neural Network is:

$$O(W_i, X_i) = \sum_{i=0}^n W_i X_i \quad (11)$$

where W_i is the weight, X_i and $O(W_i, X_i)$ denote the input and output of the model, respectively. The update rule for Adaline NN is expressed as:

$$\hat{p}(k+1) = \hat{p}(k) - \eta \frac{\partial d(k)}{\partial p} \times \frac{\partial (O(k) - d(k))^2}{\partial d} \quad (12)$$

where d and \hat{p} are the output of the IPMSM and the parameter to be estimated, respectively. η denotes the convergence speed. The Adaline NN model can be implemented given (2). For example, to estimate q-axis inductance, the corresponding equation is applied:

$$\begin{aligned} \hat{L}_q(k+1) &= \hat{L}_q(k) \\ &+ 2\eta \omega(k) i_q(k) (\hat{u}_d(k) - u_d(k)) \end{aligned} \quad (13)$$

2.5. Proposed Neural Network method

The proposed solution aims to track four machine parameters, which can take on different values at different points in time. Then, if only one Artificial NN model is employed to track the variations of all parameters, preparing the training set for that model will be difficult to achieve high generalization. Therefore, one Artificial NN model (estimator) should be used to estimate one parameter, so that for each NN model, the training set can be obtained with one parameter varied while the others are fixed.

Remark 1: As the machine parameters can vary independently, using different Artificial NN models to estimate them facilitates acquiring the training set.

Concurrently estimating 4 parameters is associated with the possibility that the variation of one parameter will affect the inputs shared among 4 NN models, which, in turn, causes wrong estimation results. Hence, the proposed solution will estimate parameters sequentially, then the variation of one parameter can be considered in estimating other parameters.

Remark 2: Sequentially estimating parameters ensures that the variation of one parameter will not affect the estimation results.

In this proposed solution, d-axis current injection is used to change the state of IPMSM, from which the machine parameters will be sequentially estimated. Given (1), the two sets of IPMSM state equations are:

$$u_{d0}(k) = -L_{q0}(k)\omega(k)i_{q0}(k) \quad (14a)$$

$$u_{q0}(k) = R(k)i_{q0}(k) + \psi_{m0}(k)\omega(k) \quad (14b)$$

$$u_d(k) = R(k)i_d(k) - L_q(k)\omega(k)i_q(k) \quad (14c)$$

$$u_q(k) = Ri_q(k) + L_d\omega(k)i_d(k) + \psi_m(k)\omega(k) \quad (14d)$$

in which, the variables and parameters with and without subscripts "0" denote the measured data when $i_d = 0$ (A) and $i_d = -2$ (A), respectively.

It is assumed that $L_{q0} = L_q$ and $\psi_{m0} = \psi_m$. The inputs to each NN model are determined from (14). For example, to estimate L_{q0} , the inputs to the corresponding NN model include $u_{d0}(k)$, $\omega(k)$ and $i_{q0}(k)$ as presented in (14a). Further, instead of feeding the inputs directly to each NN model, several tests conducted suggest that if the inputs to an NN model can be simplified, it can give better estimation results. In this proposed solution, each NN model will have one input and one output (one-to-one NN model). Therefore, there will be 4 NN models with the corresponding input/output summarized in Table 1 and the estimation process is presented in Figure 1. Specifically, when $i_d = 0$ (A), NN models to identify L_q and R are enabled, while the other two models to identify L_d and ψ_m are disabled and vice versa when $i_d = -2$ (A). It is noted that estimation process requires a time delay after current switching, which avoids the effect of current switching and ensures the stability of the estimated parameters.

Remark 3: An NN model might fail to map its inputs to a correct output, then preprocessing the inputs can improve its estimation accuracy.

Different neural network structures have been tested with different number of hidden neurons and different hidden transfer functions. Finally, one common neural network configuration is chosen for four parameter estimators, which is shown in Figure 2.

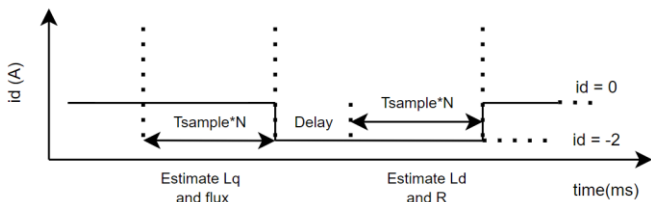


Figure 1: Estimation process based on d-axis current injection.

Table 1: NN model summary

Model	Output	Input
1	$L_{q0} = L_q$	$\frac{-u_{d0}(k)}{\omega(k)i_{q0}(k)}$
2	$\psi_{m0} = \psi_m$	$\frac{u_{q0}(k) - R(k)i_{q0}(k)}{\omega(k)}$
3	R	$\frac{u_d(k) + L_q(k)\omega(k)i_q(k)}{i_d(k)}$
4	L_d	$\frac{u_q(k) - R(k)i_q(k) - \psi_m(k)\omega(k)}{\omega(k)i_d(k)}$

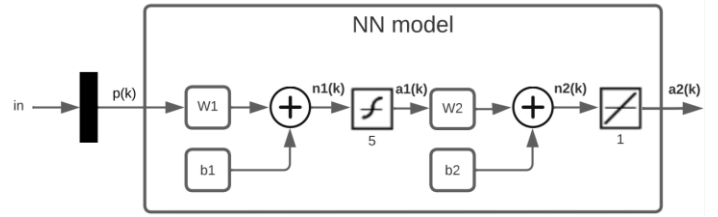


Figure 2: The common NN configuration for all parameter estimators.

A hyperbolic tangent sigmoid function is chosen as the activation function for the input and hidden layer, and relationship between its input and output of this layer can be expressed as:

$$n_1 = W_1 * p + b_1 \quad (15a)$$

$$a_1 = \text{tansig}(n_1) = \frac{2}{1 + e^{-2n_1}} - 1 \quad (15b)$$

Meanwhile, a pure linear function is chosen as the activation function for the output layer, which gives the following relationship:

$$n_2 = W_2 * a_1 + b_2 \quad (16a)$$

$$a_2 = \text{purelin}(n_2) = n_2 \quad (16b)$$

The reason for selecting the hyperbolic tangent for the input, and hidden layers is that the nonlinear hyperbolic tangent can help the model to learn more complex functions than using a linear activation function. For the output layer, the pure linear function was selected as the activation function to make the training process faster since the pure linear function does not require the update of the weight for this activation function [19].

The block diagram for the proposed solution is shown in Figure 3 which consists of 4 one-to-one NN estimators and two triggers to enable these estimators.

3. Simulation setup and results

3.1. Simulation setup

In this paper, the proposed solution is applied to a IPMSM drive system implemented in MATLAB/Simulink software, which employs Field-oriented control (FOC) algorithm. The simulation time (T_{sample}) is set at 10^{-4} s. The nominal machine parameters are presented in Table 2.

Table 2: Nominal parameters of the IPMSM motor

Parameter	Value
L_d (H)	0.045
L_q (H)	0.102
ψ_m (Wb)	0.533
R (Ω)	5.8

The d -axis and q -axis inductances of the machine were first measured experimentally by using the standstill test. These measured parameters were used to build the simulation model of the IPMSM in the Matlab/Simulink. The data used for training each NN model are collected from simulation of the IPMSM drive system at different load

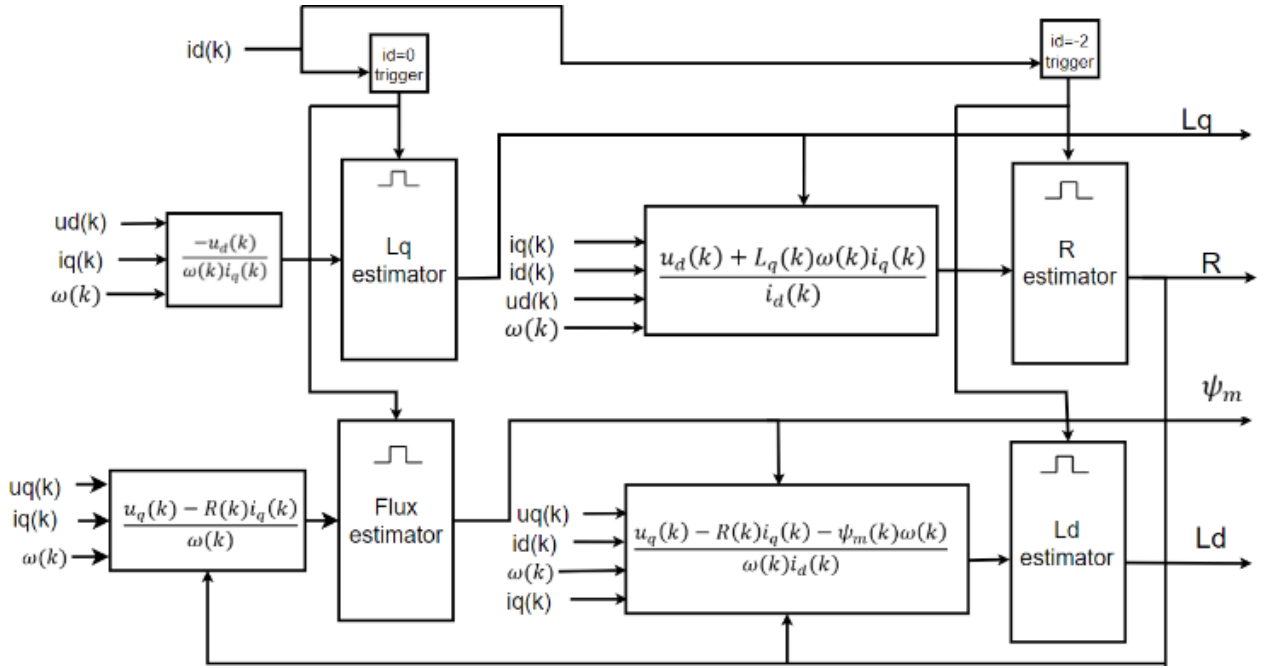


Figure 3: The proposed solution block diagram.

torques, different values of ψ_m and R . Specifically, by varying one parameter, while fixing other parameters at their nominal values, one training set is acquired. For example, the NN model to identify R is trained with the data set, in which actual R increases while the other machine parameters are fixed at their nominal values. Similar steps are repeated to acquire the training set for other three NN models. 20001 samples are collected for training each NN model with the ratio of 70:15:15 for training, validation and test sets, respectively. The number of epochs is set to 1000 and the minimum gradient is set to $1e^{-15}$ to ensure all NN models will not be underfitting. Each model performance is evaluated based on Mean Square Error (MSE) as shown in Figure 4. Furthermore, all NN models are trained with Levenberg-Marquardt back-propagation algorithm with μ is set to 0.001. According to the results shown in Figure 4, the validation and test curves are similar. This indicates the successful training processes for all estimators.

3.2. Simulation results and discussion

The performance of the proposed online parameter identification method was compared with RLS, EKF and Adaline NN. It is worth noting that the implemented EKF can only estimate R and ψ_m , while RLS and Adaline NN can estimate all four parameters. Figure 5 shows the estimation results for different techniques with constant machine parameters. In general, the outputs for all techniques converge if not considering slight fluctuations due to the effect of injected i_d signal. Further, it could be seen that the proposed NN model outperforms other three techniques in terms of estimation accuracy and convergence speed. The explanation for this is that RLS, EKF and Adaline NN require accurate inputs to produce accurate outputs. On the other hand, the proposed NN tries to map its input to the corresponding output, then the

estimation accuracy depends on how the NN model is trained instead of how accurate its input is. For example, if the dq -axis voltages are not well-compensated, RLS, EKF and Adaline NN might fail to estimate parameters. However, if the error between dq -axis voltages fed to the NN estimators and actual dq -axis voltages does not vary significantly over time, the proposed technique will produce better results as presented in Figure 5. More comprehensive test cases were conducted to further evaluate performance of the proposed solution as following:

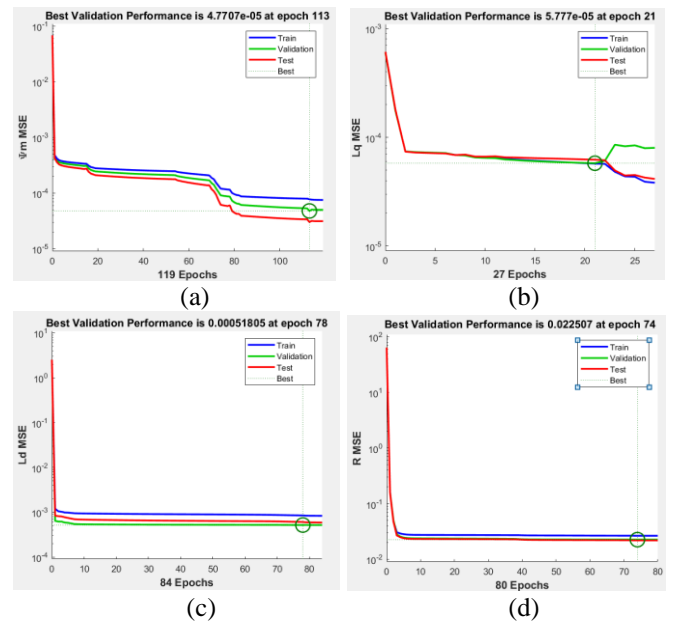


Figure 4: Learning curves for four NN estimators. (a) Flux estimator. (b) Q-axis inductance estimator. (c) D-axis inductance estimator. (d) Resistance estimator.

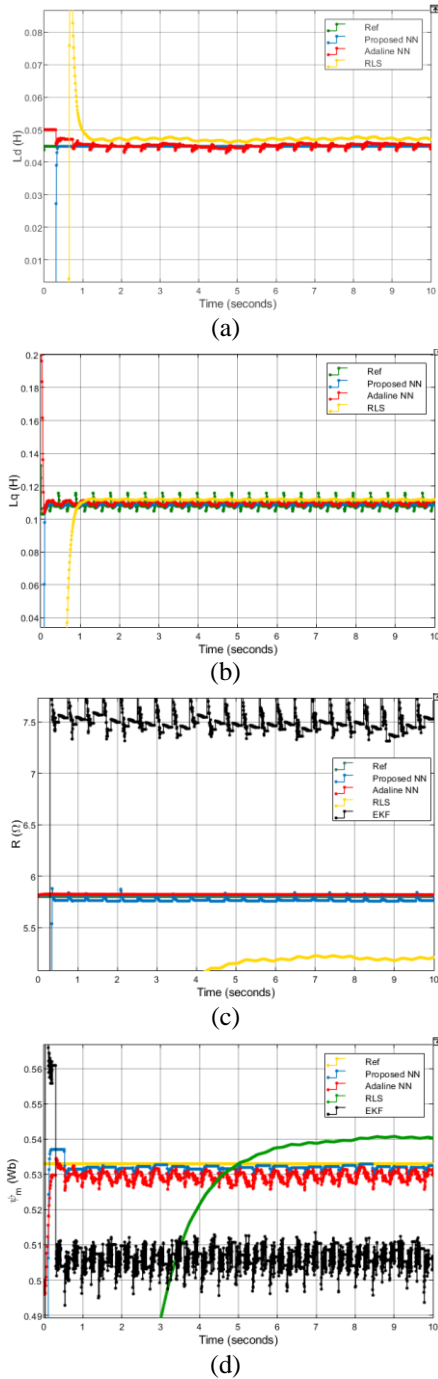


Figure 5: Estimation results for different techniques at $\omega = 1000 \text{ rpm}$ with $T = 5 \text{ N.m}$, $R = 5.8 \Omega$ and $\psi_m = 0.533 \text{ Wb}$. (a) Estimated L_d ; (b) Estimated L_q ; (c) Estimated R ; (d) Estimated ψ_m .

3.2.1. Varying load torque test

This test was conducted to verify the effectiveness of the proposed technique in tracking the variation of inductances due to varying load torque (T). The IPMSM was run at the constant speed of 1000 rpm with $R = 5.8 \Omega$, $\psi_m = 0.533 \text{ Wb}$ and during the simulation and load torque was changed from 4 to 5 N.m at around 1.05s as presented in the upper-left plot in Figure 6. Because of the d-axis current injection effect, the reference L_q shows the similar shape as a square wave, having the peak-to-peak value in the order of one thousandth, which can be negligible. After the

change in the load torque, the reference and estimated L_q agree well with each other, which are at 0.109H and 0.109H , respectively. No noticeable change in L_d can be observed from the upper-right plot in Figure 6. At the same time, the other two estimated parameters converge to their reference values.

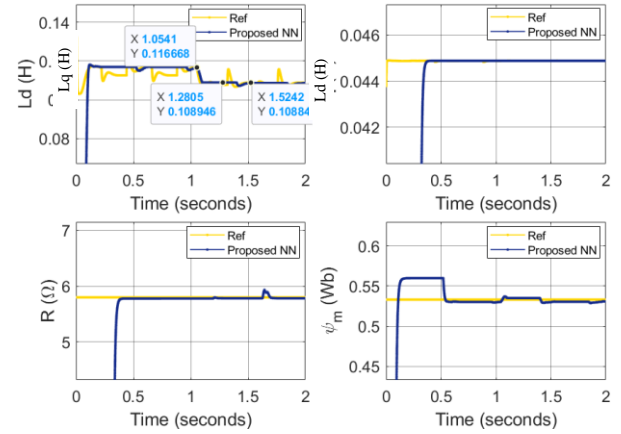


Figure 6: Estimation results for the proposed technique at $\omega = 1000 \text{ rpm}$ with load torque varying from 4 N.m to 5 N.m , $R = 5.8 \Omega$ and $\psi_m = 0.533 \text{ Wb}$.

3.2.2. Varying flux test

In this test, the IPMSM speed, R and load torque were set at 1000 rpm , 5.8Ω and 5 N.m , respectively, while only ψ_m was changed from 0.533 Wb to 0.528 Wb at around 1.19s as shown in the lower-right plot in Figure 7. At 0.69s , the estimated ψ_m converges to 0.53 Wb , which is closed to its reference value of 0.533 Wb . After 1.19s , the reference ψ_m drops to 0.528 Wb and the flux estimator can track the drop by producing the output of 0.527 Wb . The proposed method shows the small difference in the estimated and reference ψ_m .

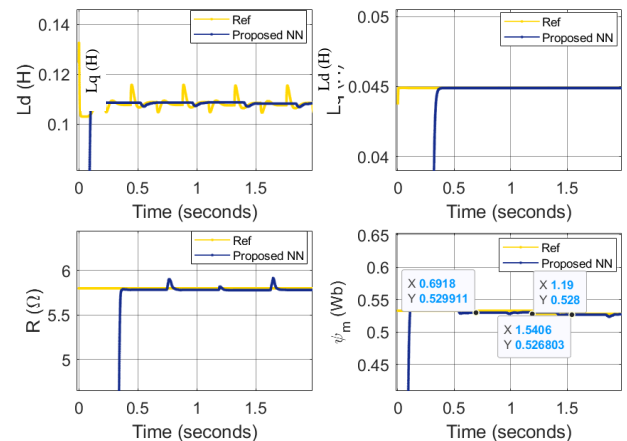


Figure 7: Estimation results for the proposed technique at $\omega = 1000 \text{ rpm}$ with ψ_m varying from 0.533 Wb to 0.528 Wb , $T = 5 \text{ N.m}$ and $R = 5.8 \Omega$.

3.2.3. Varying resistance test

The third test is to evaluate the performance of the proposed technique in tracking the variation in R . The working condition for this test was set such

that *load torque* = 5 N.m , $\psi_m = 0.533 \text{ Wb}$ and R varying from 5.8Ω to 6.3Ω at 0.91s as presented in the lower-left plot in Figure 8. At 1.5s , the cursor indicates that the estimated R lies at 6.15Ω , while its reference value is at 6.3Ω . The difference of less than 3% shows that the proposed solution has successfully track the change in R .

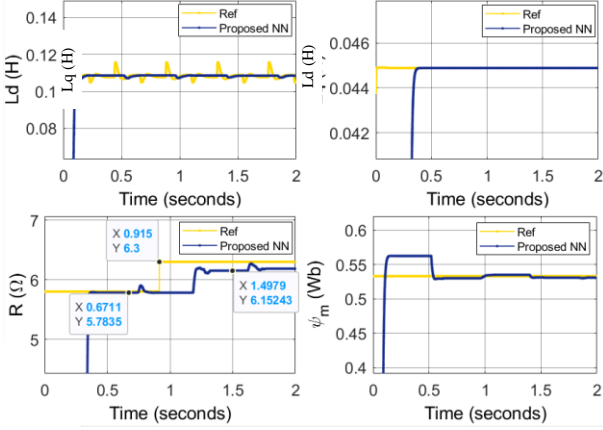


Figure 8: Estimation results for the proposed technique at $\omega = 1000 \text{ rpm}$ with R varying from 5.8Ω to 6.3Ω , $T = 5 \text{ N.m}$ and $\psi_m = 0.533 \text{ Wb}$.

3.2.4. Varying speed test

In the last test, the IPMSM was given a speed step from 700 rpm to 1000 rpm at around 1.18 s as shown in the lower-right plot in Figure 9. Meanwhile, T , R and ψ_m were set at 5 N.m , 5.8Ω and 0.533 Wb , respectively.

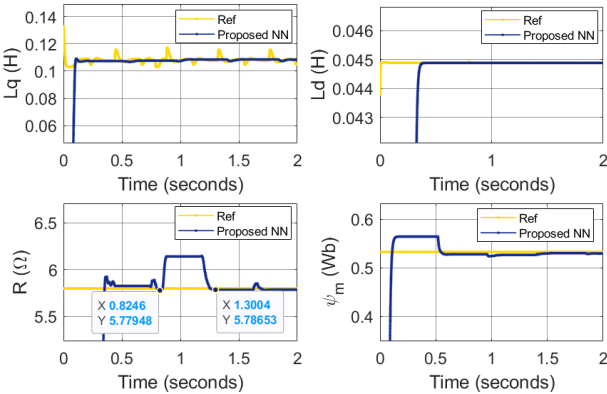


Figure 9: Estimation results for the proposed technique with $T = 5 \text{ N.m}$, $\psi_m = 0.533 \text{ Wb}$, $R = 5.8 \Omega$ and speed varying from 700 to 1000 rpm .

When the speed increases, the drive system enters transient state, which leads to a variation in the input to R estimator. As a result, there is a step change in the estimated R after 0.82s . However, at 1.3s , the estimated R drops to 5.8Ω because the system has become stable. In this test, the other estimated parameters experience no significant change due to the step change in speed. Hence, the proposed solution shows accurate estimation of all four parameters in the case of operating speed variation.

3.2.5. Discussion

The simulation results have been presented to compare the performance the EKF, RLS, Adaline NN and the proposed NN based methods in terms of the estimation accuracy and the updated time of the IPMSM' s parameters including stator resistance, d-q axis inductances and the rotor flux linkage. The performance of every method is summarized in Table 3. In general, the advantage of the EKF method is that no current injection is required. However, this method fails to estimate the variation of the machine inductances since nominal values of the machine inductances are required to develop the estimator for the stator resistance and the rotor flux linkages. This EKF method also produce low accuracy due to the effect of the non-linearity of the inverter to the accuracy of the dq- voltages. Furthermore, the update time of the estimated parameters is slow due to the recursive nature of the algorithm. The difficulty in tuning of the covariance matrices (P and Q) is also the challenge of this method. Better than the EKF method in terms of the number of estimated parameters, the RLS methods can estimate four parameters at the same time. However, the low accuracy and slow update time are the major disadvantages of this method. The reasons for these disadvantages are also the same for the EKF method, namely as non-linearity effect of the inverter and slow recursive iterations. On the other hand, the Adaline neural network is shown to be more advantageous compared to EKF and RLS in terms of the update time of the parameter. This is because the algorithm of ANN is simple and requires less computation time [4]. However, this method still suffers low estimation accuracy due to the non-linearity effect of the inverters. Finally, the proposed NN based method have been proved to be more advantageous compared to the remaining methods with high estimation accuracy and fast update capability since there is no impact of the non-linearity of the inverter to the estimator and there is no recursive iteration of the method. The machine parameters are estimated based on non-linear regression principle, of which the change of the measured input voltage and current results in a variation of the estimated parameters. The major limitation of the proposed method is the requirement for the offline model training and the variation of the parameters must be within the range of the training data.

Table 3: Performance comparison of the online parameter identification methods

Methods	R_s	L_d	L_q	ψ_m	Accuracy	Update time
EKF	Yes	No	No	Yes	Low	Slow
RLS	Yes	Yes	Yes	Yes	Low	Slow
Adaline NN	Yes	Yes	Yes	Yes	Low	Fast
Proposed	Yes	Yes	Yes	Yes	High	Fast

4. Conclusion

This paper has presented a new approach to deal with IPMSM parameter identification problems based on Artificial Neural Network model. Four neural network models have been proposed to estimate stator resistance, d-

axis, q- axis inductance and the rotor flux linkage, respectively. The input of every NN estimator is the function of the specific measured signals including estimated d-q axis voltages, measured d-q currents and the rotor speed. The simulation results have proved that the proposed technique outperforms EKF, RLS and Adaline NN methods, which require accurate signal measurement and are heavily affected by the non-linearity of the inverter. Furthermore, the proposed technique has shown its ability to effectively track the change in all parameters under the variation of load torque, speed, stator resistance and rotor flux linkage. The future work of this project will be the experimental implementation and analysis of the proposed and the conventional online parameter identification methods.

Acknowledgement

This work was supported by the Nafosted Vietnam under the grant 107.99-2019.341.

References

- [1] S. Sakunthala, R. Kiranmayi and P. N. Mandadi, "A study on industrial motor drives: Comparison and applications of PMSM and BLDC motor drives," 2017 International Conference on Energy, Communication, Data Analytics and Soft Computing (ICECDS), 2017, pp. 537-540, doi: 10.1109/ICECDS.2017.8390224.
- [2] H. P. Huy Anh, P. Quoc Khanh and C. Van Kien, "Advanced PMSM Machine Parameter Identification Using Modified Jaya Algorithm," 2019 International Conference on System Science and Engineering (ICSSE), 2019, pp. 445-450, doi: 10.1109/ICSSE.2019.8823434.
- [3] K. Liu and Z. Q. Zhu, "Position-Offset-Based Parameter Estimation Using the Adaline NN for Condition Monitoring of Permanent-Magnet Synchronous Machines," in *IEEE Transactions on Industrial Electronics*, vol. 62, no. 4, pp. 2372-2383, April 2015, doi: 10.1109/TIE.2014.2360145.
- [4] Z. Q. Zhu, D. Liang and K. Liu, "Online Parameter Estimation for Permanent Magnet Synchronous Machines: An Overview," in *IEEE Access*, vol. 9, pp. 59059-59084, 2021, doi: 10.1109/ACCESS.2021.3072959.
- [5] M. S. Rifaq and J. Jung, "A Comprehensive Review of State-of-the-Art Parameter Estimation Techniques for Permanent Magnet Synchronous Motors in Wide Speed Range," in *IEEE Transactions on Industrial Informatics*, vol. 16, no. 7, pp. 4747-4758, July 2020, doi: 10.1109/TII.2019.2944413.
- [6] G. Wang et al., "Self-Commissioning of Permanent Magnet Synchronous Machine Drives at Standstill Considering Inverter Nonlinearities," in *IEEE Transactions on Power Electronics*, vol. 29, no. 12, pp. 6615-6627, Dec. 2014, doi: 10.1109/TPEL.2014.2306734.
- [7] Y. S. Chen, "Motor topologies and control strategies for permanent magnet brushless AC drives," Ph.D. dissertation, Univ. Sheffield, Sheffield, U.K., 1999
- [8] F. Khatounian, S. Moreau, E. Monmasson, A. Janot, and F. Louveau, "Parameters estimation of the actuator used in haptic interfaces: Comparison of two identification methods," in *Proc. IEEE Int. Symp. Ind. Electron.*, vol. 1, Jul. 2006, pp. 211-216
- [9] K. M. Rahman and S. Hiti, "Identification of machine parameters of asynchronous motor," *IEEE Trans. Ind. Appl.*, vol. 41, no. 2, pp. 557-565, Mar. 2005.
- [10] K. Liu and Z. Q. Zhu, "Online estimation of the rotor flux linkage and voltage-source inverter nonlinearity in permanent magnet synchronous machine drives," *IEEE Trans. Power Electron.*, vol. 29, no. 1, pp. 418-427, Jan. 2014.
- [11] K. Liu and Z. Q. Zhu, "Position-offset-based parameter estimation using the Adaline NN for condition monitoring of permanent-magnet synchronous machines," *IEEE Trans. Ind. Electron.*, vol. 62, no.4, pp. 2372-2383, Apr. 2015.
- [12] J. H. Feng, "Fault diagnosis method of traction motor bearing based on improved flux peak energy spectrum," *J. Central South Univ.*, early access, pp. 1-9, Jul. 2020. [Online]. Available: <http://kns.cnki.net/kcms/detail/43.1426.N.20200727.1016.002.html>
- [13] M. A. Mazzoletti, G. R. Bossio, C. H. De Angelo, and D. R. Espinoza-Trejo, "A model-based strategy for interturn shortcircuit fault diagnosis in PMSM," *IEEE Trans. Ind. Electron.*, vol. 64, no. 9, pp. 7218-7228, Sep. 2017.
- [14] K. Liu, Q. Zhang, J. Chen, Z. Q. Zhu and J. Zhang, "Online Multiparameter Estimation of Nonsalient-Pole PM Synchronous Machines With Temperature Variation Tracking," in *IEEE Transactions on Industrial Electronics*, vol. 58, no. 5, pp. 1776-1788, May 2011, doi: 10.1109/TIE.2010.2054055.
- [15] B. N. Mobarakeh, F. Meibody-Tabar, and F. M. Sargos, "Mechanical sensorless control of PMSM with online estimation of stator resistance," *IEEE Trans. Ind. Appl.*, vol. 40, no. 2, pp. 457-471, Mar./Apr. 2004
- [16] R. Ramakrishnan, R. Islam, M. Islam, and T. Sebastian, "Real time estimation of parameters for controlling and monitoring permanent magnet synchronous motors," in *Proc. IEEE Int. Elect. Mach. Drives Conf.*, Miami, FL, USA: IEEE, 2009, pp. 1194-1199
- [17] X. Liu and Y. Du, "Torque Control of Interior Permanent Magnet Synchronous Motor Based on Online Parameter Identification Using Sinusoidal Current Injection," *IEEE Access*, vol. 10, pp. 40517-40524, 2022, doi: 10.1109/ACCESS.2022.3167041
- [18] X. Li and R. Kennel, "Comparison of state-of-the-art estimators for electrical parameter identification of PMSM," 2019 IEEE International Symposium on Predictive Control of Electrical Drives and Power Electronics (PRECEDE), 2019, pp. 1-6, doi: 10.1109/PRECEDE.2019.8753197.
- [19] Goodfellow, I.; Bengio, Y. & Courville, A. (2016), *Deep Learning*, MIT Press .